IAA-AAS-DyCoSS2-13-04

GNSS BASED ATTITUDE DETERMINATION SYSTEMS FOR NANOSATELLITES

Vincenzo Capuano,[*] Cyril Botteron,[†] and Pierre-André Farine [‡]

Attitude determination systems based on global navigation satellite systems (GNSSs) present several advantages, most of all, for very small satellites. GNSS receivers have low power consumption, limited mass, small volume, and are relatively inexpensive. However, if the attitude information is extracted from the relative position between two or more GNSS antennas placed on the nanosatellite, due to the small baseline between them, the achievable accuracy will not be as good as the one obtained with other high performance attitude sensors. In order to circumvent the accuracy limitation, an alternative single-antenna GNSS-based method is presented, which estimates attitude information through the use of the GNSS-derived accelerations.

I. INTRODUCTION

The use of commercial satellite imagery is growing rapidly, and has numerous applications in meteorology, agriculture, geology, forestry, landscape, biodiversity conservation, regional planning, education, intelligence and warfare. Satellite imagery is also used in seismology and oceanography in deducing changes to land formation, water depth and sea bed, to detect earthquakes, volcanoes, and tsunamis.[1] Earth imaging has typically been based on large and expensive satellite platforms. However, driven by the increasing miniaturization of electronics and MEMS technology, Earth imaging is potentially also becoming achievable with very small satellites.[2] Because of their low costs, short development periods, standardizations, and applicability to various space missions, the use of small satellites such as CubeSats instead of a large platforms results to be very convenient and cost-effective also for Earth imaging[2]. For example, while the total cost for five large Earth Imaging satellites construction and launch is approximately 50.000.000 €, the cost to build and launch 10 6U CubeSats is just 5.306.667 € [3], i.e., about an order of magnitude less. At the same time, since the very early days of satellite imagery, pointing accuracy and attitude stability have been key parameters of the satellite design. Indeed, an inaccurate pointing could prevent keeping the target in the camera field of view (FOV), while coarse attitude stability would make the images blurred. However, because of strict constraints such as low power consumption, low mass and limited volume, the development of a precise and accurate Attitude Determination System (ADS) for very small satellites is very challenging. For instance, it is difficult to integrate precise gyro sensors such as Fiber Optic gyroscope and Ring Laser gyroscope in a CubeSat, because of the above mentioned constraints and also due to their prohibitive costs for a CubeSat mission. For these reasons, there is therefore a growing interest in GNSS-based ADSs, as GNSS receivers are relatively inexpensive, have low power consumption, limited mass, small volumes, low installation costs and most importantly, a GNSS-based ADS is driftless. In order to compute the attitude, it is possible to use

[*] Mr., ESPLAB, École Polytechnique Fédérale de Lausanne (EPFL), Switzerland, vincenzo.capuano@epfl.ch.
[†] Dr., ESPLAB, École Polytechnique Fédérale de Lausanne (EPFL), Switzerland, cyril.botteron@epfl.ch.
[‡‡] Prof., ESPLAB, École Polytechnique Fédérale de Lausanne (EPFL), Switzerland, pierre-andre.farine@epfl.ch.

GNSS code observations or carrier-phase observations, from a single antenna or from multiple ones. Although GNSS code observations may be used to estimate an attitude solution, generally, carrier phase observations are preferred because they can increase the accuracy by roughly two orders of magnitude.[4] With three not collinear antennas that form two baselines, the full attitude can be determined. Unfortunately, the achievable accuracy will be limited by the baseline length, and for a very small satellite, the distance at which the antennas can be placed is restricted by the size and geometry of the satellite itself. Thus, because of the small baseline, a multiple-antenna configuration for nanosatellites results in an accuracy not as high as for larger platforms. Furthermore, the use of more than one antenna incurs a complex structure, large volume, and high cost of the attitude determination system.

In order to remove the antenna baseline length dependence and save volume, mass, costs, and reduce complexity, we evaluate in this paper the achievable performance of a single-antenna GNSS receiver that estimates attitude information through the use of GNSS-derived acceleration vector in the Earth Centered Inertial (ECI) frame. This vector can be calculated by double-differentiating the carrier phase or by differentiating directly the GNSS velocity to obtain the range acceleration vector. On the other hand, the receiver acceleration vector in the Body Reference Frame (BRF) can be measured using a three-axis accelerometer. Then, by combining the ECI acceleration vector and the BRF acceleration vector with another pair of vectors, provided e.g. by a magnetometer (which measures the geomagnetic field vector in the BRF) and by an onboard geomagnetic field model (which provides the geomagnetic field vector in the ECI), it is possible to extract the rotation matrix of the host satellite, as Wahba's problem solution. It is shown that the resultant attitude uncertainty would be less than 2° on average.

This paper is organized as follows: Section II characterizes briefly the main attitude determination sensors and technologies currently available on the market based on their attitude determination accuracy, mass, power and cost. Section III describes the attitude determination technique, commonly known as *deterministic point by point solution*, which estimates the attitude from at least two (or preferably more) reference vectors, observed at a single point in time. In section IV several GNSS-based attitude determination methods are discussed, which rely on the *deterministic point by point solution*. Section IV.I and section IV.II describe respectively the multiple-antenna and single antenna approaches. Section V reports the simulation models used to estimate the accuracy of the attitude partial information, extractable from the single antenna measurements and the corresponding simulation and experimental results. Finally, section VI describes the full attitude accuracy achievable when the GPS derived accelerations are fused with accelerometers and magnetometer measurements.

II. SENSORS CURRENTLY AVAILABLE ON THE MARKET

Figure 1 illustrates some characteristics of the attitude determination sensors typically adopted for nanosatellites. In particular, as well as the observable, the accuracy, the mass and the cost are reported as an average of the values corresponding to several products currently available on the market.[5,6,7]

As described in (Reference 8), the cheapest configuration and furthermore the most common for a nanosatellite ADS consists of a three axis Magnetometer, a minimum number of Sun Sensors (sufficient to ensure the Sun is in one FOV) and a three axis MEMS Gyro. This can be seen as a *basic configuration*. The first two sensors work together to provide two different vector observations, which can be used as inputs to solve the Wahba's problem (described in section III): in this way, outside eclipse, when the sun sensors can work, it is possible to extract the full attitude. The three axis MEMS Gyro provides the angular velocity, which can be integrated to obtain the attitude during the eclipse orbital part, when the sun sensors cannot work. The biggest disadvantage of the Gyro is the "angular random walk" (ARW). This is the white noise component of the *drift*, which has units of $\frac{deg}{\sqrt{hour}}$ or $\frac{deg}{\sqrt{seconds}}$. . It can be thought as the variation (or standard deviation), due to noise, of the result of integrating the output of a stationary gyro over time. For example we can consider a gyro with an ARW of $1°/\sqrt{second}$, being integrated many times to derive an angular position measurement. Being proportional to the square root of the integration time, this ARW would be 1° after 1 second and 10° after 100 seconds.[9] Therefore, gyros have to be calibrated often. In (Reference 8), for the *basic configuration*, the achieved accuracy outside eclipse is limited by the ECI geomagnetic field vector

prediction (due to the coarse geomagnetic model on board) and during the eclipse the accuracy decreases over time because of the drift-ARW effect, reaching approximately 8°. Thus, this *basic configuration* can be seen as relatively inexpensive (considering the total cost even lower than that one for a single star tracker) but it does not provide the attitude with the required high-accuracy necessary for several applications, such as e.g. Earth imaging.

An alternative to the Sun Sensors, could be the Earth Horizon Sensors. These sensors have the drawback that they cannot operate when the satellite is in eclipse if they operate in the visible range of the electromagnetic spectrum and they can just provide pitch and roll measurements.

The Star Tracker is currently the attitude sensor with the highest performance but it is expensive and for this reason most of times it may not be compatible with low cost development requirements. Moreover, although becoming smaller, Star Trackers are typically not suitable for nanosatellites because of their high power consumption and their large and heavy baffles.

GNSS receivers are not present in Figure 1. Observable, accuracy, weight, power, and price of the attitude determination sensors typically used for nanosatellites. The provided information is an average of the values *corresponding to* several products currently available *on the market.*

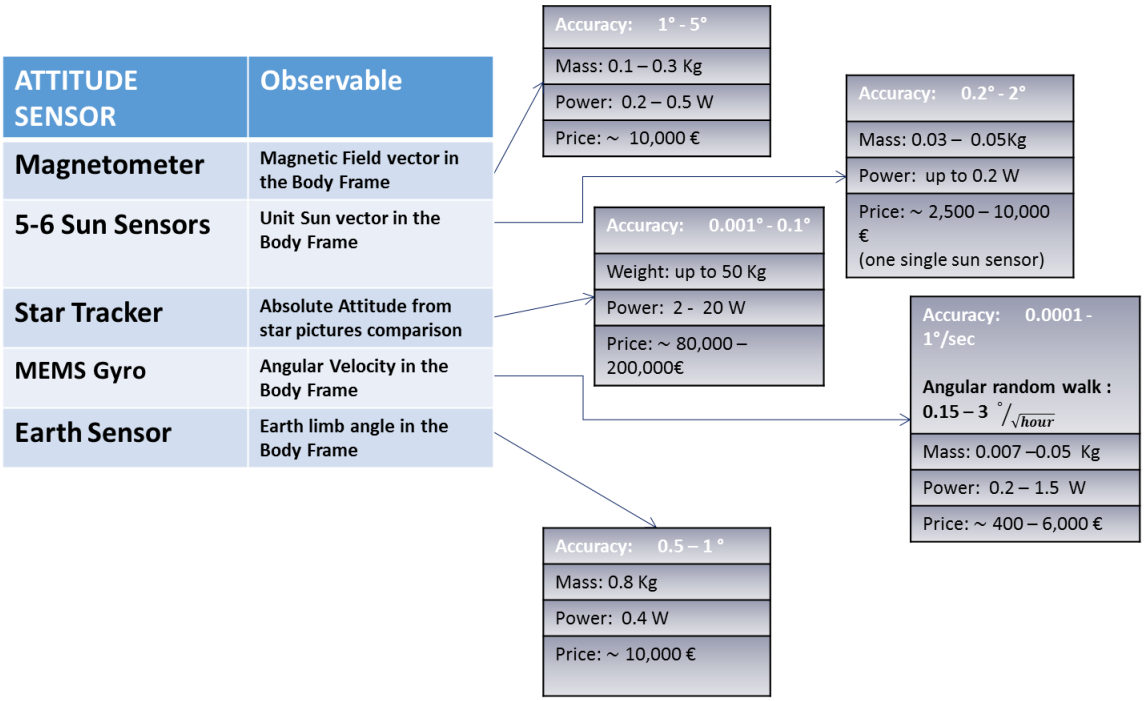

Figure 1. Observable, accuracy, weight, power, and price of the attitude determination sensors typically used for nanosatellites. The provided information is an average of the values corresponding to several products currently available on the market.

III. ATTITUDE DETERMINED BY REFERENCE VECTORS

Reference vector sensors use references such as the Earth, the Sun or the Stars to provide vector information.[11] If these vectors are measured with the respect to the BRF and simultaneously predicted with the respect to the ECI, it is possible to extract information about the body orientation (attitude). In fact, if one unit vector $\boldsymbol{v}$ is known in the BRF as $\boldsymbol{v}_{BRF}$ and also in the ECI as $\boldsymbol{v}_{ECI}$, it implies that $\boldsymbol{v}_{ECI} = R_{BRF}^{ECI}\boldsymbol{v}_{BRF}$, where R_{BRF}^{ECI} is the rotation matrix that transforms the vector $\boldsymbol{v}$ expressed in the BRF $\boldsymbol{v}_{BRF}$, in the vector v expressed in the ECI $\boldsymbol{v}_{ECI}$. At least two pairs of unit vectors $\boldsymbol{v}_{BRF}, \boldsymbol{v}_{ECI}$ and $\boldsymbol{u}_{BRF}, \boldsymbol{u}_{ECI}$ are required to determine the attitude R_{BRF}^{ECI}, because the latter is defined (as rotation matrix or equivalently as unit quaternion) by three independent parameters, while a unit vector $\boldsymbol{v}$ by two independent ones. One of the simplest ways to estimate the spacecraft attitude, given two pairs of vectors $\boldsymbol{v}_{BRF}, \boldsymbol{v}_{ECI}$ and $\boldsymbol{u}_{BRF}, \boldsymbol{u}_{ECI}$, is the TRIAD algorithm, due to Harold D. Black in 1964, well described in (Reference 12). But most of the attitude determination methods using simultaneous vector measurements are based on a problem introduced in 1965 by Grace Wahba, known as Wahba's problem. The Wahba's problem solution is a rotation matrix *R* between two coordinate systems. In the case of attitude determination, the matrix is calculated from a set of (weighted) vectors observations $\boldsymbol{v}_{BRF_i}$ in the BRF (which are the measurements provided by sensors like i.e. magnetometer and sunsensors), and from the same vectors $\boldsymbol{v}_{ECI_i}$ predicted in the ECI by an on board model. As described in (Reference 12), the Wahba's problem solution is a optimal estimation because it minimizes the following cost function:

$$J(R) = \frac{1}{2}\sum_{i=1}^{m} a_i \left\| \boldsymbol{v}_{BRF_i} - R_{ECI}^{BRF}\boldsymbol{v}_{ECI_i} \right\|^2 \qquad m \geq 2 \qquad (1).$$

Where a_i are scalar weights assigned to each vectors set.

Figure 2 shows the principle above described when the two unit vectors are provided by a three axis Magnetometer and a Sun Sensor. The direction of the Sun respectively in the BRF and in the ECI is indicated as $\hat{\boldsymbol{s}}_{BRF}$ and $\hat{\boldsymbol{s}}_{ECI}$ and the direction of the local geomagnetic field as $\hat{\boldsymbol{m}}_{BRF}$ and $\hat{\boldsymbol{m}}_{\boldsymbol{ECI}}$. R_{ECI}^{BRF} is the rotation matrix from the ECI to the BRF.

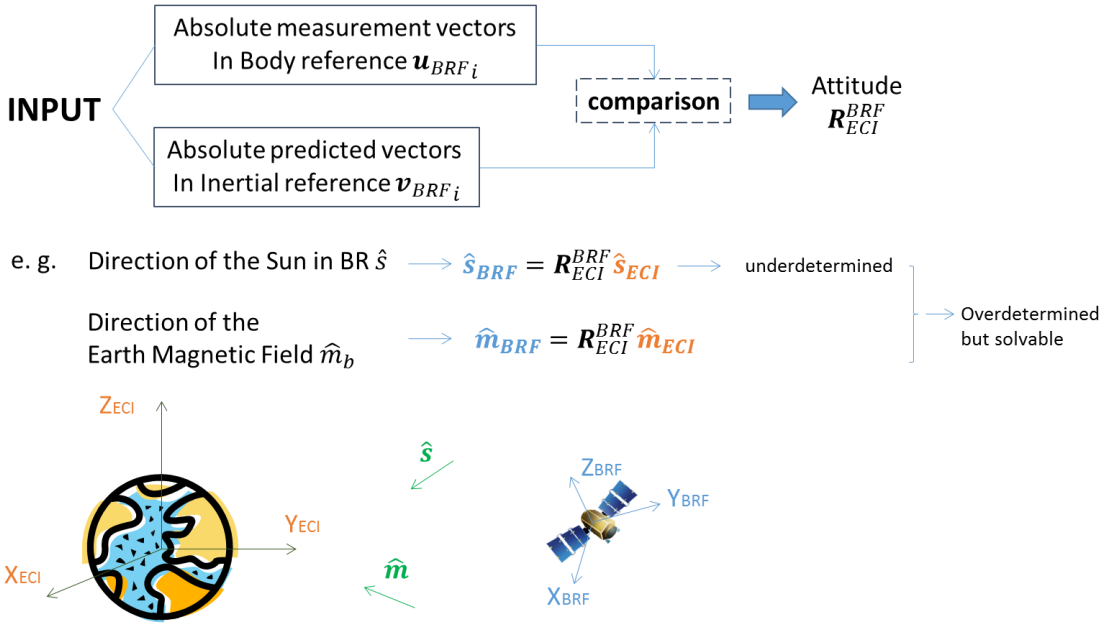

Figure 2. Attitude determined by two unit vectors.

IV. GNSS BASED ATTITUDE DETERMINATION

Global Positioning System (GPS), the most popular GNSS, was originally designed as a three dimensional radio position, navigation and time system for land, sea and airborne users. In order to determine position and time, the user just needs a receiver to capture and process signals from at least four GNSS satellites of the system constellation. Later, GNSS has been used for many other applications like surveying and mapping, weather prediction improvements, etc. However, nowadays, among numerous applications, GNSS is also used as attitude determination system. As already mentioned, it is possible to use GNSS code observations or carrier-phase observations from a single or multiple antennas to derive attitude information.[13] In sections IV.I and IV.II respectively a multiple antenna and a single antenna configuration are analysed.

IV.I Multiple Antenna Approach

The measurements of the carrier phase from two antennas placed on a body, allow to determine the angle of arrival (AOA) in the Body Reference Frame (BRF). This method is commonly classified as phase interferometer direction finding.[14] The principle is illustrated in Figure 3 for the simple case of two antennas. The GNSS signal AOA is equal to: [15]

$$\vartheta = \cos^{-1}\left(\frac{N+\frac{\Delta\varphi}{2\pi}}{d}\cdot\lambda\right) \qquad (2).$$

Where $N\lambda + \frac{\Delta\varphi}{2\pi}\lambda$ corresponds to the projection of the baseline d on the line of sight (LOS). Thus, we can see that the AOA is related to the phase difference. In fact, except when the incident signal is perpendicular to the antennas baseline, the phase measurements of the incoming GNSS signal carrier are different for each antenna, because they are located in different positions. By measuring $\Delta\varphi$ and calculating the integer number of cycles N travelled by the carrier, it is possible to estimate ϑ. The accuracy depends primarily on three factors: GNSS observation quality, AOA itself and the length of the baseline between the antennas.[4] Unfortunately, for very small satellites, the distance at which the antennas can be placed is limited by the size and geometry of the satellite itself. An upper-bound for the ϑ achievable accuracy may be obtained by calculating its Cramer-Rao Lower Bound (CRLB).

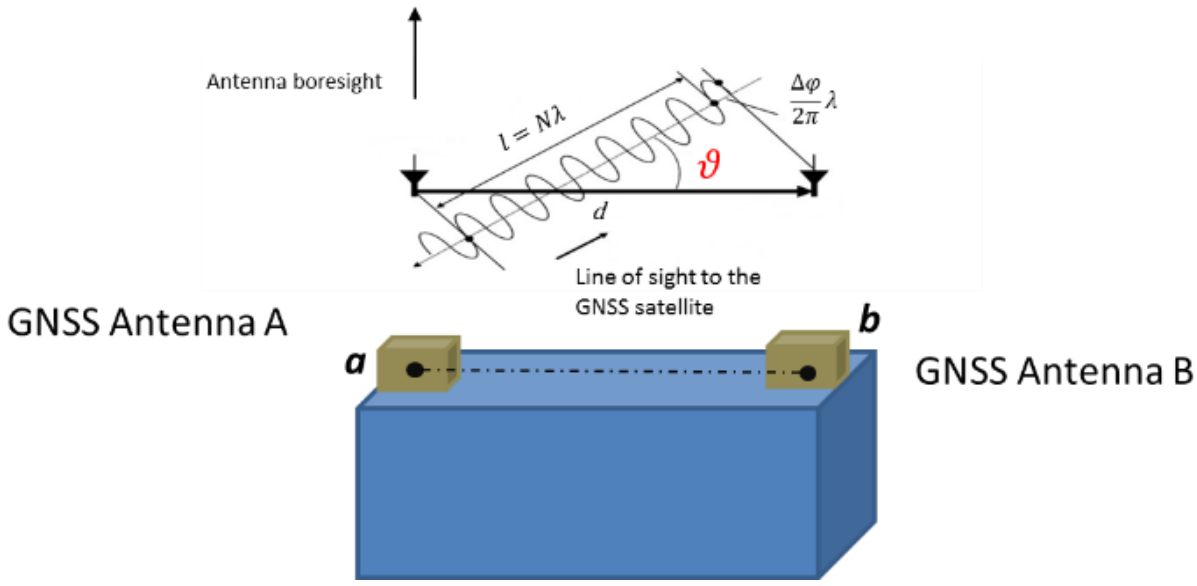

Figure 3. Phased Interferometer DF working principle.

Mathematically, we have two measurement data sets $\{\varphi_1, \varphi_2\}$, which depend on an unknown parameter ϑ that is the AOA. We want to determine ϑ based on the data. This is equivalent to define an estimator:

$$\hat{\vartheta} = g(\varphi_1, \varphi_2).$$

This is a problem of parameter estimation. The CRLB provides a lower bound for the mean square error (MSE) of any unbiased estimator for an unknown parameter (ϑ).[16] By assuming that the GNSS satellites transmitters radiate a sinusoidal signal, we can express the received signal at the *n*th antenna (for $n \in \{a, b\}$) as $A\cos(2\pi F_0(t - t_n) + \varphi)$ where t_n is the propagation time to the *n*th antenna. For LEO altitudes the two antennas are located enough far from the target, such as the signal circular wavefront can be considered to be planar at the two antennas. The wavefront at the antenna *a* lags the one at the antenna *b* by $d\frac{\cos\vartheta}{c}$, where c is the signal propagation speed, due to the extra propagation distance $d\cos\vartheta$. Then, if the propagation time to the antenna *a* is t_a, the propagation time to the antenna *b* will be $t_b = t_a - d\frac{\cos\vartheta}{c}$. Thus, the observed signal at the antenna *b*, is:

$$s_b(t) = A\cos\left[2\pi F_0\left(t - t_a + d\frac{\cos\vartheta}{c}\right) + \varphi\right] \qquad (3).$$

By assuming that the sensors output are corrupted by white Gaussian noise, from (Reference 16) the CRLB of ϑ is:

$$var(\vartheta) \leq \frac{12}{(2\pi)^2 6\, SNR\left(\frac{d}{\lambda}\right)^2 (\sin\vartheta)^2} \qquad (4).$$

where $\lambda = \frac{c}{F_0}$ is the wavelength of the propagating signal and SNR is its Signal-to-Noise Ratio.

By considering λ = 19 cm for GPS L1, d = 9 cm for a CubeSat and an SNR of 20 dB, reasonable value in LEO,

$$var(\vartheta) \in [0.01°, 1°], \text{ for } \vartheta \in [85°, 5°] \text{ respectively.}$$

In order to determine the full attitude, at least three antennas not collinear are necessary. In fact, three GNSS antennas can be used to measure the direction of arrival (DOA) of a GNSS signal, from two independent AOA measurements ϑ_1 and ϑ_2 as shown in Figure 4. A DOA corresponds to the unit vector in the BRF representing the signal direction of the corresponding GNSS satellite. This vector can be calculated in the ECI from the GNSS satellites ephemeris (part of the GNSS data message). At least two simultaneous GNSS satellites are necessary to calculate the attitude by using equation (1).

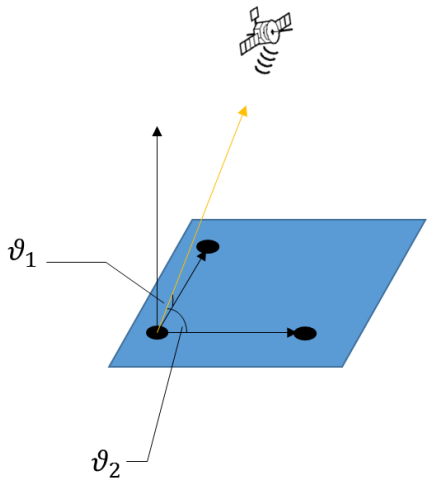

Figure 4. Two independent AOA of the GNSS signal, defined by three antenna (two baselines).

Then, the basic idea it to use the GNSS receiver as a traditional reference sensor described in section II, whose observable is a unit vector, exactly like e.g. for Magnetometer or a Sun Sensor. The considerable advantage is that the GNSS reference sensor is able to provide the full attitude autonomously, thanks to the number of GNSS satellites available, which for Low Earth Orbit (LEO) is more than two.[17] The need of at least two GNSS satellites can be also explained in this way: while for position determination at least four GNSS satellites need to be "visible", for attitude determination only two GNSS satellites are necessary; in fact the four unknowns (platform coordinates and receiver clock offset) are reduced to two unknowns because of the common time reference for each antennas and the relative antennas position already known a priori.[4] The more GNSS satellites will be available, the more accurate will be the attitude estimation because the higher will be the number of contributions in the cost function (1), where the weights could be proportional to the signal to noise ratio of each signal and/or to the relative position to the other satellites. Figure 5 illustrates the principle here discussed. Other marked advantages is that the GNSS reference sensor would be able to work during the whole orbit, including the eclipse phase and moreover it is completely driftless.

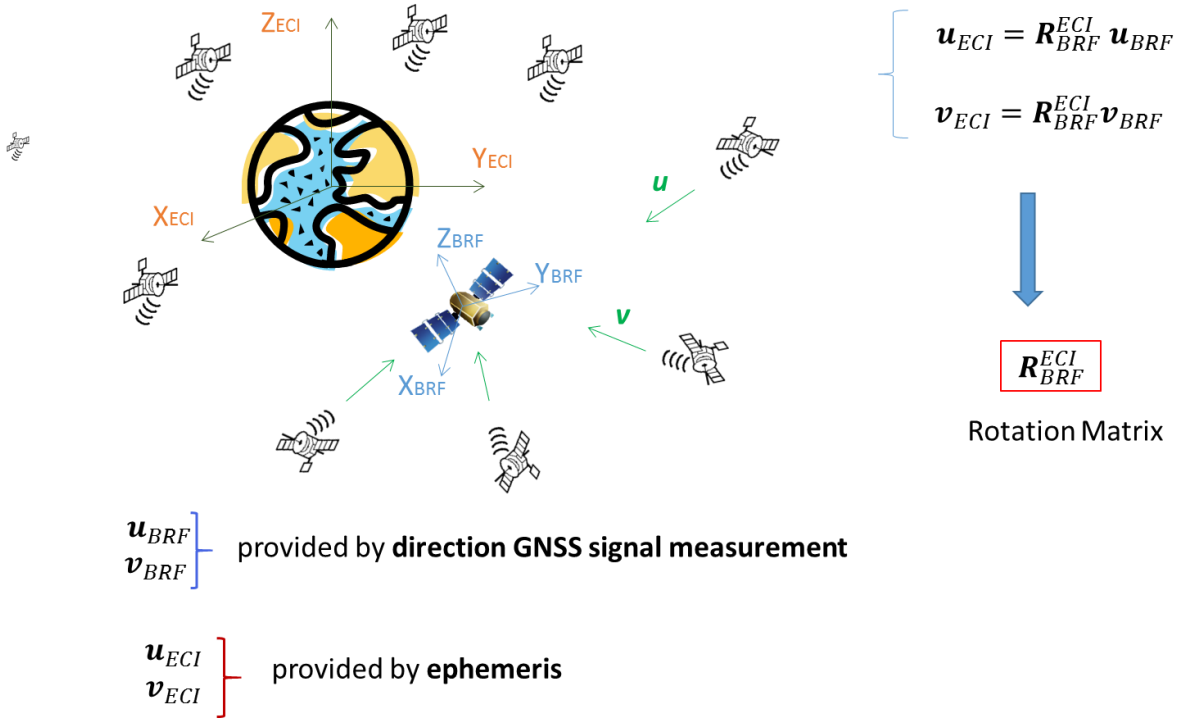

Figure 5. Attitude determined by GNSS signals direction and ephemeris broadcasted in the GNSS message.

Although the CRLB of the phase interferometer AOA has been roughly estimated to be within 1°, from (References 4) the accuracy σ_R of the full attitude *R*, determinable by carrier phase measurements from multiple antennas, can be roughly estimated as follows:

$$\sigma_R = ADOP \cdot \frac{\sigma_{range}}{d}\ (rad) \qquad (5).$$

Where:

d	is the baseline length,
σ_{range}	is error in range,
$ADOP = \sqrt{trace[(nI - SS^T)^{-1}]}$	is the Attitude Dilution of Precision, similarly to the Geometry Dilution of Precision (GDOP), and I the identity matrix
$S = [s_1, s_2, \ldots s_n]$	is the matrix 1 x n of unit vectors s_i,
s_i	is the LOS to the satellite *i*,
n	is the number of satellites in view.

Generally $ADOP \leq 1$ and thus, as proposed in (Reference 18 and 19), by making the approximation of ADOP = 1,

$$\sigma_R = \frac{\sigma_{range}}{d} \qquad (6).$$

In (References 4), from an analysis on the different sources of errors in range (multipath, structural distortion, troposphere, SNR and error in the receiver), multipath results to be the dominant error, as also stated in (Reference 18 and 19). Furthermore, previous investigations[20] showed that even with the most careful study on the location of the antenna, the error cannot be reduced below 5 *mm*.

Thus, for a baseline of 10 cm for CubeSats, an approximation of σ_R could be:

$$\sigma_R = \frac{5}{d} = \frac{5}{100} = 0.05\ rad = 2.86°.$$

IV.II Single Antenna Approach

The use of more than one antennas incurs a more complex structure, a larger volume, and higher cost of the attitude determination system. Moreover, the attainable accuracy with small baselines is not as high as with long baselines. These characteristics restrict its application for nanosatellites. Instead, a single antenna GNSS receiver can be used as a multi-purpose navigation sensor to provide attitude information in addition to position and velocity measurements.

Signal Strength Measurements

The first GNSS observable used in most single antenna attitude systems was the signal strength measurement: by assuming that the receiving antenna gain reduces monotonically from the boresight vector to 90° off-boresight and that the azimuthal gain variation is enough small to be ignored, through the measurement of all GNSS satellite signal strengths and the known geometry of the tracked satellites, the orientation of the antenna boresight vector, with respect to a reference coordinate system, can be estimated, as proposed i.e. in (Reference 21, 22, 23 and 24). In one approach developed by the *NASA Jet Propulsion Laboratory* (JPL) in 1998, the antenna boresight direction (that corresponds to the single-axis solution) is estimated as the weighted average of the line-of-sight (LOS) vectors from the GPS receiver antenna to each tracked GPS

satellite. Each weight is assigned based on the measured Carrier-to-Noise ratio C/NO value, in such way that the GPS satellites corresponding to the higher C/NO measurement will have the higher weight applied to their LOS vector. But the achievable accuracy was coarse: for six to eight tracked GPS satellites was approximately 15°.[23] In a second approach, developed by Axelrad in (Reference 21), the received GPS signal strength is modelled as a function of the boresight angle, from which a single-axis solution is obtained. For this approach, the achieved accuracy was demonstrated to vary between 3.2° and 11.9° rms for space-borne data, and between 10° and 15° for ground data. For both mentioned approaches the main cause of the coarse accuracy is the inaccurate modeling of the GPS signal transmission link budget parameters.[23] However if the measured C/NO value is modelled as function of the antenna boresight angle only, not enough information are available for a full 3-axis attitude solution, which can be obtained if i.e. the antenna boresight model is coupled with a magnetometer measurement, as proposed in (Reference 24). In (Reference 24), it is shown that using a single antenna on a gradient stabilized satellite, by implementing a three dimensional receiving antenna gain model, the full 3-axis attitude determination is possible, however the potential accuracy is of the order of 3° for pitch and roll and 10° for yaw. In a more recent work described in (Reference 24), 5-7° RMS accuracy are demonstrated in simulation by using single antenna GPS SNR observations coupled with a magnetometer.

GNSS Derived Acceleration

Another way to extract attitude information from a single GNSS antenna is through the use of the GNSS derived acceleration. This can be implemented by differentiating doubly the carrier phase[25] or by differentiatinng directly the GNSS velocity[26] to obtain the range acceleration. GPS-derived acceleration can be used as an absolute attitude reference if coupled with with a 3-axis accelerometer. The GNSS derived acceleration vector, combined with the gravity vector and the centrifugal and Coriolis effects of the Earth's rotation, provides the estimation of a vector that corresponds to the equivalent of a 3-axis accelerometer output in the Earth-centered, Earth-fixed (ECEF) frame. In fact, an on board 3–axis accelerometer provides the same vector in the BRF. This two vectors couple can be used with another vectors couple provided by an on board magnetometer and an on board geomagnetic field model, in order to solve the Wahba's problem and provide the full attitude. In this paper, we estimate firstly the GPS derived acceleration (obtained by differentiating the ECEF GNSS velocity) and after, the attitude determination accuracy achievable by using these accelerations and the ones provided by accelerometers in conjunction with a magnetometer and a dipole geomagnetic model. The ECEF accelerations $\boldsymbol{a}_{ECEF}$ can be estimated by time differentiating the ECEF velocity $\boldsymbol{v}_{ECEF}$ provided as standard output of a GNSS receiver through the carrier frequencies Doppler shifts measurements of the GNSS satellites signal. Previous studies on GPS velocity determination prove that the achievable accuracies is of a few millimeters per second depending on receiver quality, whether in static or kinematic mode, stand-alone or relative mode, and the particular dynamics situation.[27,28,29]

V. GPS DERIVED ACCELERATION ACCURACY

The GPS ECEF derived acceleration $\boldsymbol{a}_{ECEF}$ accuracy is calculated by using:

- the ECEF velocity observations $\boldsymbol{v}_{ECEF}^{GPS}$ provided as standard output of the "*U-Blox 5 GPS engine*" receiver;
- the GPS L1 signal generated by the very accurate multi-GNSS full constellation simulator "*Spirent GSS8000*";
- the observed ECEF accelerations $\boldsymbol{a}_{ECEF}^{GPS}$, obtained by time differentiating the $\boldsymbol{v}_{ECEF}^{GPS}$;
- the true velocities $\boldsymbol{v}_{ECEF}^{true}$ and true accelerations $\boldsymbol{a}_{ECEF}^{true}$ provided by the "*Spirent GSS8000*" simulator, for which the corresponding signal is generated.

Since the "*U-Blox 5 GPS engine*" is limited to work within 50 Km of altitude[30], the ECEF velocity observations $\boldsymbol{v}_{ECEF}^{GPS}$ have been obtained for the following cases:

- *Static Earth user*. The "*U-Blox 5 GPS engine*" receives the GPS L1 signal from "*Spirent GSS8000*" simulator, which generates the signal that the receiver would receive if it was placed on the Earth surface at longitude East 6°56.4', latitude North 46°59.4' and altitude 400 m (Neuchatel, Switzerland), on April 10th 2013, at 12:15.
- *Dynamic airborne user*. The "*U-Blox 5 GPS engine*" receives the GPS L1 signal from "*Spirent GSS8000*" simulator, which generates the signal that the receiver would receive on April 1st at 10:00, if it was placed on board an aircraft, which, from the starting point at latitude 50°25.21', longitude -4°5.994' and height 140 m, performs the following flight maneuver:
    - slow acceleration - 20 s duration - speed change of 60 m/s
    - Climb – height change 300 m, height rate 8m/s, lateral acceleration start 1 g, lateral acceleration end 1.5 g
    - Acceleration Turn – heading change 125°0', lateral acceleration start 1 g, lateral acceleration end 1.5 g, speed change 30 m/s
    - acceleration – duration 120 s, speed change 120 m/s
    - Straight – duration 950 s.

To calculate the tropospheric delay, the Spirent simulator uses the tropospheric model from (Reference 32). The ionospheric delay is modelled according to the Klobuchar model.[33] The constellations model consists of 31 GPS satellites, including at least four satellites in each of six orbital planes, as described in (Reference 33). In this study just the L1 GPS is considered, for which it is assumed a power reference level of -130 dBm.

Figure 6 and Figure 7 illustrate the velocity measurement error histogram, obtained by comparing the "*U-Blox 5 GPS engine*" ECEF velocity observations $\boldsymbol{v}_{ECEF}^{GPS}$ to the corresponding true $\boldsymbol{v}_{ECEF}^{true}$ provided by "*Spirent GSS8000*", for the *Static Earth user* and the *Dynamic airborne user* cases.

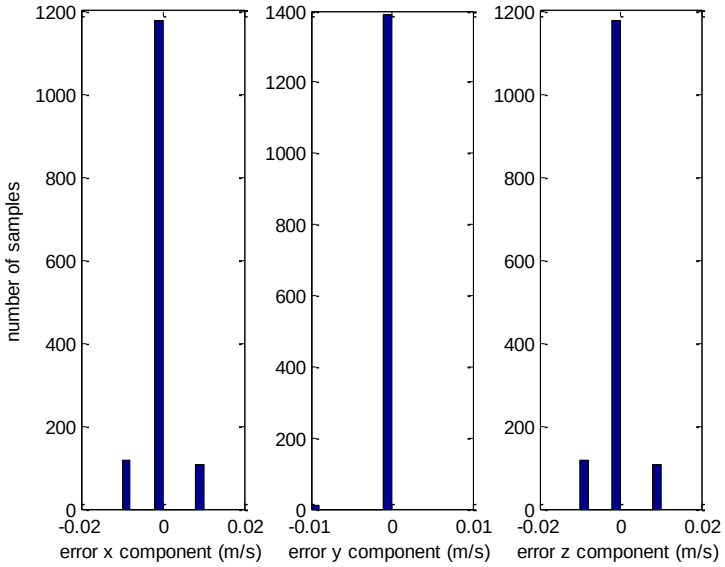

Figure 6. Velocity measurement error histogram of the "*U-Blox 5 GPS engine*" for the *Static Earth user* case.

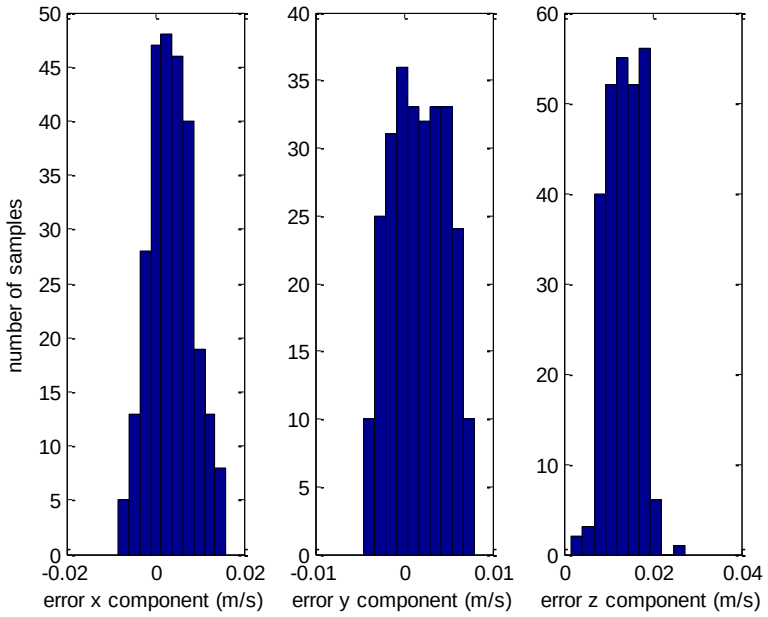

Figure 7. Velocity measurement error histogram of the "*U-Blox 5 GPS engine*" for the *Dynamic airborne user* case.

By time-differenting the ECEF velocity observations $\boldsymbol{v}_{ECEF}^{GPS}$, the corresponding observed ECEF accelerations $\boldsymbol{a}_{ECEF}^{GPS}$ are computed. The $\boldsymbol{a}_{ECEF}^{GPS}$ are then compared to the true accelerations $\boldsymbol{a}_{ECEF}^{true}$ provided by the "*Spirent GSS8000*" simulator obtaining the observed acceleration error vector $\boldsymbol{e}_{ECEF}^{a}$. Figure 8 and Figure 9 respctively shows the histogram of the Cartesian components of $\boldsymbol{e}_{ECEF}^{a}$, for the *Static Earth user* and for the *Dynamic airborne user* cases.

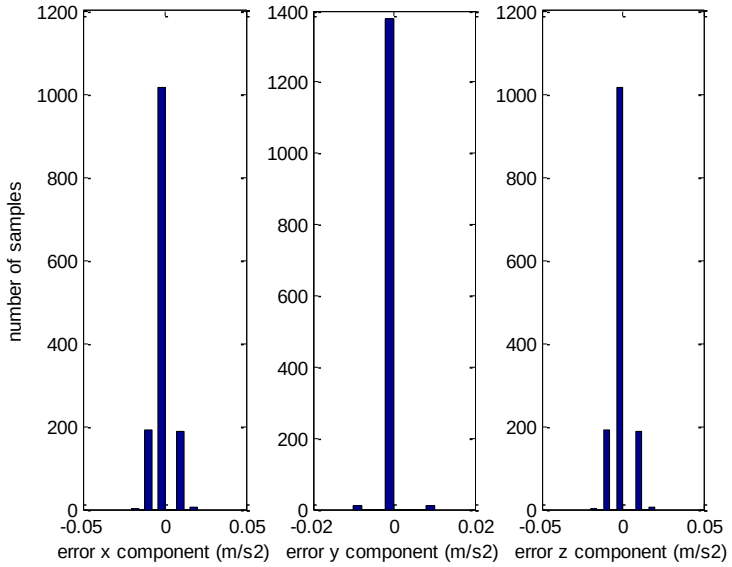

Figure 8. Acceleration error histogram for the *Static Earth user* case.

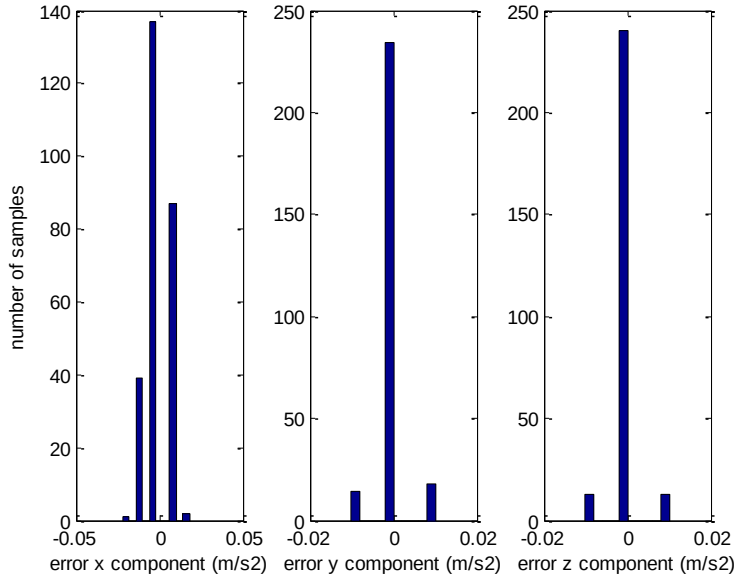

Figure 9. Acceleration error histogram for the *Dynamic airborne user* case.

For the the *Static Earth user* case the acceleration error has a standard deviation of 0.005 m/s in the x and z component, 0.001 m/s in the y component , while for the *Dynamic airborne user* case 0.007 m/s in the x, 0.004 m/s in the y and 0.003 m/s in the z component.

The corresponding attitude information accuracy can be calculated as arc cosine of the dot product between the $\boldsymbol{a}_{ECEF}^{GPS}$ and the $\boldsymbol{a}_{ECEF}^{true}$ vector directions. It is illustrated in Figure 10 for the *Dynamic airborne user* case. The same information is reported as histogram in Figure 11.

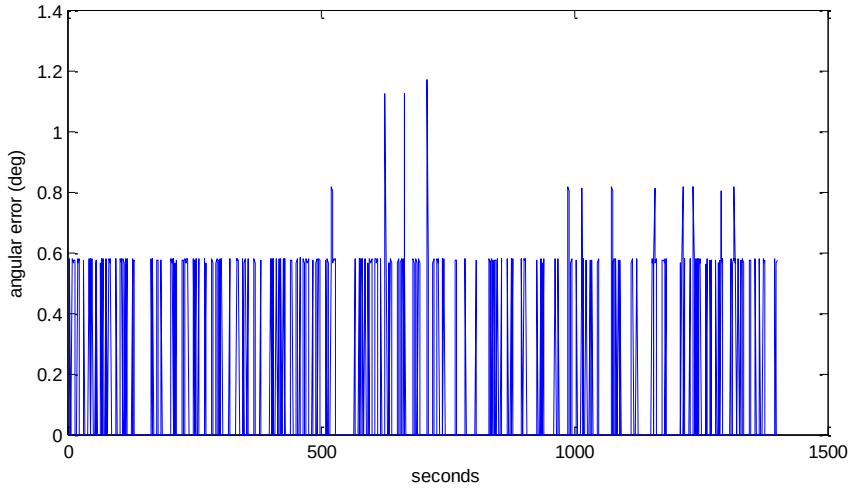

Figure 10. Attitude information accuracy obtainable from the "*U-Blox 5 GPS engine*" derived accelerations, calculated as arc cosine of the dot product between the a_{ECEF}^{GPS} and the a_{ECEF}^{true} vector directions.

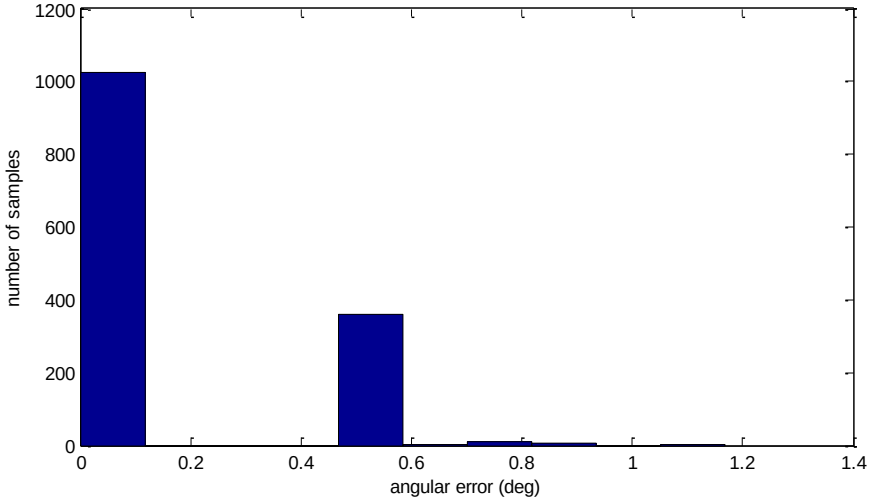

Figure 11. Histogram of the attitude information error obtainable from the "*U-Blox 5 GPS engine*" derived accelerations, calculated as arc cosine of the dot product between the a_{ECEF}^{GPS} and the a_{ECEF}^{true} vector directions.

The precision of many values in Figure 10 is due to the quantization of the GPS velocity measurement, which impact the acceleration computation and accordingly its angular error. The average angular error of less than 0.6° shows that the GPS derived accelerations can be used efficiently as attitude reference.

The GPS derived ECEF accelerations $\boldsymbol{a}_{ECEF}^{GPS}$ can provide an attitude information, but they cannot provide the full attitude; they need to be coupled to the corresponding BRF accelerations $\boldsymbol{a}_{BRF}^{INS}$ measured by accelerometers and fused with another pair of vectors $\boldsymbol{v}_{BRF}, \boldsymbol{v}_{ECEF}$ as described in section III.

VI. GPS DERIVED ACCELERATION BASED ADS

By assuming a normal distribution of the GPS derived acceleration error components, the standard deviation from the *Dynamic airborne user* test is used to model the observed ECI acceleration vector $\boldsymbol{a}_{ECI}^{GPS}$ in LEO. In order to provide the full attitude, this vector is fused with:

- the observed BRF acceleration vector $\boldsymbol{a}_{BRF}^{INS}$, measured by a three-axis accelerometer, Inertial Navigation System (INS)
- the observed BRF magnetic field vector $\boldsymbol{m}_{BRF}^{TAM}$, measured by a three-axis magnetometer (TAM)
- the predicted ECEF magnetic field vector $\boldsymbol{m}_{ECI}^{WMM2010}$, calculated by the the geomagnetic model World Magnetic Model 2010 (WMM2010).

Figure 12 illustrates the high level Simulink® architecture of the $\boldsymbol{a}_{ECI}^{GPS}$, $\boldsymbol{a}_{BRF}^{INS}$, $\boldsymbol{m}_{ECI}^{WMM2010}$, $\boldsymbol{m}_{BRF}^{TAM}$ fusion, where the Wahba's problem solution is computed by using the Singular Value Decomposition (SVD) method, which is faster than the q-method for two vector observations and more robust than other faster methods, such as FOAM and ESOQ.[11]

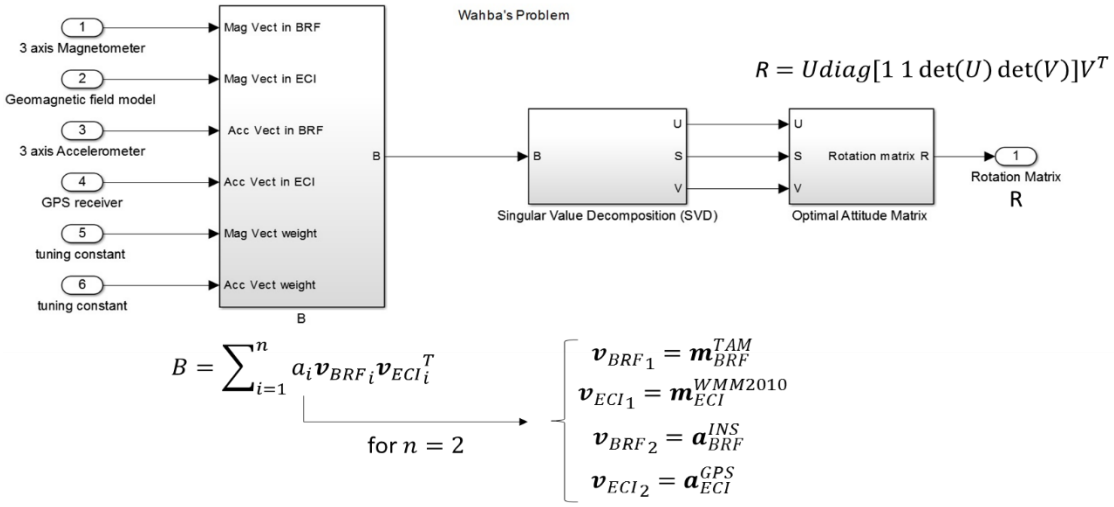

Figure 12. Simulink® ADS architecture.

The INS three-axis accelerometer output A_{meas} has been modelled as suggested in (Reference 34):

$$A_{meas} = A_{imeas} + A_{bias} + noise.$$

Where :

A_{imeas} is the ideal measured acceleration modelled as:

$$A_{imeas} = A_b + \omega_b \times (\omega \times d) + \dot{\omega}_b \times d$$

A_{bias} are the biases

ω_b are body-fixed angular rates

$\dot{\omega}_b$ are body-fixed angular accelerations

d is the lever arm

g is the gravity acceleration

In this model the following parameters have been assumed:

$$A_{bias} = \begin{bmatrix} 3.5 \\ 3.5 \\ 4.0 \end{bmatrix} mg$$

$$d = \begin{bmatrix} d_x \\ d_y \\ d_z \end{bmatrix} = \begin{bmatrix} 0 \\ 0 \\ 5 \end{bmatrix} cm$$

$$\textit{Center of gravity} = \begin{bmatrix} x \\ y \\ z \end{bmatrix} = \begin{bmatrix} 0 \\ 0 \\ 0 \end{bmatrix} cm$$

$$\textit{Noise power} = \begin{bmatrix} 0.001 \\ 0.001 \\ 0.001 \end{bmatrix}, \text{ assuming low cost accelerometers.}$$

The TAM output simulates the output of the *MAG magnetometer*[35] produced by the *SSBV Space and Ground Systems Ltd* company, taking into account its resolution of 25nT , its noise of 2nT (RMS) and a sampling rate of 10 Hz.

The WMM2010 error prediction has been modelled to be within 140nT for the North and East component and within 200nT for the Down component, as indicated in (Reference 36).

The simulated orbital scenario is summarized below:

- Semi major Axis: 7014.3 km
- Eccentricity: 0.000
- Inclination: 98 deg
- Longitude of Ascending Node: 0 deg
- Argument of Perigee: 0 deg.
- Mean Anomaly: 0 deg.

The attitude determination error corresponds to a rotation (rotation error), which is equivalent to a single rotation φ around one axis $\hat{\boldsymbol{e}}$ that runs through a fixed point as illustrated in Figure 13. Figure 14 illustrates the final attitude error expressed as angle φ of the rotation error.

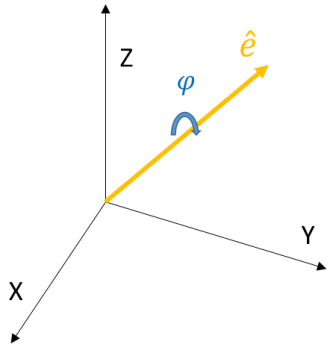

Figure 13. The rotation error.

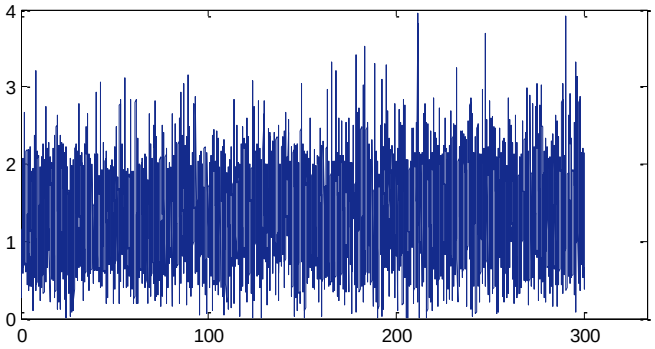

Figure 14. Final attitude error expressed as angle φ of the rotation error.

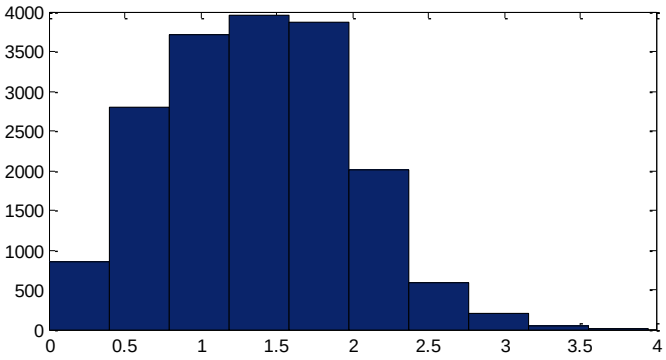

Figure 15. Histogram of the final attitude error expressed as angle φ of the rotation error.

The simulated final error has a standard deviation of 0.6°, a mean of 1.36°, and a peak of 3.95°.

VII. CONCLUSION

In addition to its original use as timing and positioning system, GNSS can also be exploited as an attitude reference system because it can provide reference vectors that can be used as input of *deterministic point by point solution* algorithms. If a multiple antenna configuration is used, from carrier phase measurements, GNSS can be used as a complete attitude determination system, autonomous and driftless. However, in this case at least three antennas have to be placed in such a way to define two very precise and accurate baselines. Moreover, the use of more than one antenna incurs a complex structure, large volume, high cost, and while the achievable accuracy can be approximately 0.1° with large baseline[14], it is reduced by more than one of order of magnitude with small baselines. A single antenna configuration seems to be more convenient for very small satellites, such as pico- and nanosatellites, which require low volume, low complexity on board systems. Although a single antenna GNSS receiver cannot provide the full attitude, it does not require special design; a GNSS receiver used on board as timing and positioning system, can in addition be used as attitude reference without any hardware modifications. The single antenna approach based on the GNSS derived accelerations can provide a much higher accuracy than the technique based on the signal strength. The accelerometers required to provide the BRF acceleration are already commonly available on board any class of satellites, because part of the on board IMU; furthermore, the Magnetometer is also very often used on board very small satellites because also required for the magnetic actuators functioning, used as main actuators of the Attitude Control System (ACS) or to desaturate reaction wheels of the same ACS. For the scenarios assumed, a mean attitude error of 1.36° makes the GNSS derived acceleration method as suitable for low cost pico- and nanosatellites missions, which do not require a very high pointing accuracy. Such a GNSS solution could also be used to provide a reference in a monitoring system or a first attitude approximation to initialize a more accurate attitude estimation.

REFERENCES

1. http://en.wikipedia.org/wiki/Satellite_imagery, October 7th 2013.

2. J. Tuthill, "Design And Simulation Of A Nanosatellite Attitude Determination System", December 2009.

3. C. Doughan, "Business Case for a CubeSat-based Earth Imaging Constellation", http://spacebusinessblog.blogspot.ch/2011/05/business-case-for-cubesat-based-earth.html, May 31st 2011.

4. R. Sabatini, L. Rodriguez, A. Kaharkar, C. Bartel, T. Shaid, "Carrier-phase GNSS Attitude Determination and Control System for Unmanned Aerial Vehicle Applications", *ARPN Journal of Systems and Software*, November 2012.

5. http://www.cubesatshop.com/index.php?option=com_virtuemart&Itemid=69, March 2014.

6. *Blue Canyon Technologies*, October 2013.

7. *Berlin Space Technologies*, October 2013.

8. V. Capuano, "Attitude Determination System for Very Small Satellites Using Data Fusion", *IAA-CU-13-05-04*, February 2013.

9. http://www.sensorwiki.org/doku.php/sensors/gyroscope, October 2013.

10. http://www.ssbv.com/ProductDatasheets/page39/page26/index.html, March 2013.

11. K. F. Jensen, K. Vinther, "Attitude Determination and Control System for AAUSAT3", 2010.

12. C. Hall, lecture notes of "Spacecraft Dynamics and Control", chapter four, *Attitude Determination*, March 18th 2003.

13. C. Lopez, GMV, "Attitude Determination", www.navipedia.net/index.php?title=Attitude_Determination&oldid=11381#Application_Examples , GMV, *Navipedia*, October 2013.

14. http://www.phys.hawaii.edu/~anita/new/papers/militaryHandbook/sig-sort.pdf, October 2013.

15. G. Giorgi, P. J. G. Teunissen, "GNSS Carrier Phase-Based Attitude Determination", February 2012.

16. S. M. Kay, "Fundamentals of Statistical Signal Processing, Estimation Theory", 1993.

17. V. Capuano, C. Botteron, P. A. Farine, "GNSS Performances for MEO, GEO and HEO", International Astronautical Congress (IAC) 2013, Beijing (China), September 2013.

18. E. D. Kaplan, C. J. Hegarty, "Understanding GPS, Principles and Application", Second Edition, 2006.

19. Cohen, C. E., "Attitude Determination Using GPS", PhD Thesis, Stanford University, 1992.

20. B. W. arkinson, "G error analysis." Global Positioning System: Theory and Applications, AIAA, vol. pp. 469-483. 1996.

21. P. Axelrad, P. C. Behre, "Satellite Attitude Determination Based on GPS Signal-to-Noise Ratio", Proceedings of the IEEE, 1999.

22. S. M. Stewart, G. N. Holt, "Real Time Attitude Determination of A Nanosatellite Using GPS Signal-To-Noise Ratio Observations", *University of Texas at Austin*, 2003.

23. C. Wang, R. A. Walker, M. P. Moody, "Single Antenna Attitude Algorithm for Non-uniform Antenna Gain Patterns, Cooperative Research Centre for Satellite Systems", *Queensland University of Technology*, Brisbane, QLD, 4000, Australia, 2003.

24. P. J. Buist, Y. Hashida, M. Unwin, "Full Attitude Determination From A Single GPS Antenna: Demonstration Of Concept With Orbital Data From Posat-1*", Delft Univeristy of Technology*, 1998.

25. Y. Li, "MEMS and Platform Orientation & Deep Integration of GNSS/Inertial Systems", *GNSS Solutions*, January/February 2008.

26. M. L. Psiaki, S. P. Powell, P. M. Kinter, "The Accuracy of the Gps-Derived Acceleration Vector, a Novel Attitude Reference*",* AIAA-99-4079.

27. Van Graas, F. and A. Soloviev, "Precise Velocity Estimation Using a Stand-Alone GPS Receiver", *Proceedings of ION NTM* 2003, Anaheim, California, 22-24 January 2003.

28. Ryan, S., G. Lachapelle and M. E. Cannon, "*DGPS Kinematic Carrier Phase Signal Simulation Analysis in the Velocity Domain*", Proceedings of ION GPS 97, Kansas City, Missouri, 16-19 September 1997.

29. L. Serrano, R. B. Langley, "A GPS Velocity Sensor: How Accurate Can It Be? – A First Look", *ION NTM 2004*, January 2004, San Diego, CA.

30. U-blox 5, NMEA, *UBX Protocol Specification*, GPS.G5-X-07036-E, 23 Dec 2008.

31. Spirent, *Simgen Software User Manual*, issue 4-02SR02, 13th December 2012.

32. NATO Standard Agreement STANAG 4294 Issue 1.

33. ICD-GPS-200F Navstar GPS Space Segment/User Segment Interfaces (21 September 2011).

34. Rogers, R. M., "Applied Mathematics in Integrated Navigation Systems", AIAA Education Series, 2000.

35. http://www.cubesatshop.com/index.php?page=shop.product_details&flypage=flpage.tpl&product_id=90&category_id=7&option=com_virtuemart&Itemid=69, July 2012.

36. S. Maus, S. Macmillan, S. McLean, M. Nair, C. Rollins, B. Hamilton, A. Thomson, "The US/UK World Magnetic Model for 2010-2015".